Journal of Organometallic Chemistry 694 (2009) 1138–1143

Contents lists available at ScienceDirect

Journal of Organometallic Chemistry

journal homepage: www.elsevier.com/locate/jorganchem

The coordination chemistry of gold surfaces: Formation and far-infrared spectra of alkanethiolate-capped gold nanoparticles

Janet Petroski [1], Mei Chou, Carol Creutz *

Chemistry Department, Brookhaven National Laboratory, P.O. Box 5000, Upton, NY 11973-5000, United States

ARTICLE INFO

Article history:
Received 28 July 2008
Received in revised form 31 October 2008
Accepted 7 November 2008
Available online 2 January 2009

Dedicated to Professor Dr. Ch. Elschenbroich on the occasion of his 70th birthday.

Keywords:
Gold nanoparticles
Capping mode
Far IR
Thiol hydrogen

ABSTRACT

We find that hydrogen is formed (slowly) in the reaction of "naked gold" with thiols in toluene, thereby establishing the fate of a significant fraction of the thiol H when thiols react with gold nanoparticles to yield monolayer-protected clusters. The far-infrared spectra of 2-nm alkane–thiolate-capped Au nanoparticles have been determined in order to probe the binding of alkanethiols (pentane, hexane, decane, dodecane, hexadecane, and octadecane) to the particle surface. Bands due to the Au–S stretch were observed in the range 170–270 cm^{-1}, with most samples exhibiting two bands in this region. The Au–S stretch frequencies observed here are similar to those found from HREELS of alkanethiol SAMs on Au(1 1 1) (J. Phys. Chem. B 106 (2002) 9655) and are consistent with recent descriptions of the surface as being stabilized by Au(I)-bridged thiolate "staples" (Science 318 (2007) 407).

1. Introduction

Self-assembled monolayers (SAMs) of thiols on gold and other metals are widely used to tailor the surfaces of crystals/electrodes and nanoparticles under a wide range of synthetic conditions [1,2]. Gold nanoparticles capped with alkanethiols have been studied extensively [3,4]. There is now general agreement [3] that this capping material is bound as "thiolate" R–S, although instances are known in which some of the coordination sites are occupied by thiol R–SH [5]. For a 2-nm nanoparticle an Au–S bond length of 2.31 Å has been inferred from X-ray absorption fine structure spectroscopy (EXAFS) studies [6]. A combined EXAFS/transmission electron microscopy (TEM) study indicates thiolate-binding to a threefold site and an Au–S distance of 2.31 Å, with ca. two-thirds of the surface Au atoms bound to RS [7]. However, much confusion has remained as to the nature of the metal–thiolate bond and the nature of the thiol adsorption process in both two-dimensional (SAM) and three-dimensional (nanoparticle assemblies). Denoting the Au SAM or nanoparticle as $Au_n(Au–S–R)_m$ where the Au_n are in the bulk or core and Au_m are on the surface, an oxidative adsorption mechanism (e.g. Eq. (1))

$$Au_{n+m} + m\ RSH \rightarrow Au_n(Au{-}S{-}R)_m + mH^+ + me^- \quad (1)$$

has been invoked for spontaneous self-assembly [8,9] and for the electrochemically assisted formation of thiol SAMs on Au [10,11] and Pt [12]. (For the former case dioxygen or adventitious impurities serve as oxidant; for the latter, the oxidation is electrochemical). In addition there is evidence for

$$Au_{n+m} + m\ RSH \rightarrow Au_n(Au{-}S{-}R)_m + m/2\ H_2 \quad (2)$$

conversion of thiol H to dihydrogen [1,2]. On the other hand, in HREELS studies of methanethiol on Au(1 1 1), the SH stretch was detected, indicating binding of thiol, not thiolate [13]. In temperature-programmed-desorption studies of alkanethiols on Au(1 1 1) H_2 was found to desorb below the desorption temperature of the parent thiol for octanethiol (at 280 K), but not for lower thiols [14]. In 2002 Hasan et al. detected bound S–H by proton NMR on 2–5-nm particles and provided the first direct evidence for this bonding mode on nanoparticles [5]. The approach used exploited "place-exchange" of thioether ligands, which, unlike thiols, provide no suitable site for the H of the incoming thiol.

What has remained unclear is whether in the preparation of SAMs or monolayer-protected clusters, the thiol H is lost as H^+, as $H^+ + e^-$ by reaction with O_2, or as H_2. For self-assembled monolayers, the amount of material – and hydrogen gas that would be evolved – are very small, complicating any determination of the amount of hydrogen produced. In contrast, the availability of high-surface-area nanoparticles in mg-g quantities provides an opportunity for a conventional analytical approach to hydrogen determination. For example, for "naked gold" particles stabilized

* Corresponding author.
E-mail address: ccreutz@bnl.gov (C. Creutz).
[1] Present address: Chemistry Dept., Loyola College, 4501 N. Charles St., Baltimore, MD 21201, United States.

0022-328X/$ - see front matter © 2008 Elsevier B.V. All rights reserved.
doi:10.1016/j.jorganchem.2008.11.057

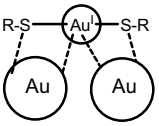

Fig. 1. R–S–Au–S–R "staple" adapted from Ref. [23].

by tetraoctylammonium bromide (TOAB), the fraction of Au atoms on the surface ranges from 25% (5 nm particles of 3800 total with 950 atoms on the surface) to 60% (2-nm particles of 300 total Au atoms with 180 on the surface). In the present work, we report determination of H_2 from the reaction of "naked gold" nanoparticles with octadecanethiol and 4-methylthiophenol by gas chromatography under reaction conditions similar to those of the Brust et al. [15] synthesis, except that no aqueous phase containing sodium borohydride is present.

In the second part of this study we use far-infrared spectroscopy to probe the binding of thiolate to the surface of 2-nm Au nanoparticles. Though many studies have examined the properties of the hydrocarbon portion of the capping material and the self-assembly of the nanoparticles, the Au–S bond itself has received less attention. Previous IR and Raman studies [16–18] of gold nanoparticles and self-assembled monolayers focused on the structural defects of the alkanethiol chain seen in the mid-IR range and not the sulfur binding. Characterization of the Au–S bond by far-IR spectroscopy offers the possibility of elucidating the nature of surface interaction with this ligand and of also probing the nature of the surface of the nanoparticle itself, since information on the environment of the surface gold atoms can be extracted. Such an examination is particularly relevant in the context of recent structural studies that have led to revision of the description of these surfaces. Thus, a model of the clusters and SAMs as a metallic gold core encapsulated by a gold thiolate oligomers –SR–Au–SR– or –SR–AuSR–Au–SR) is emerging [19]. Recent studies of octanethiol [20] and benzenethiol [21] bonding to Au(111), probed by scanning tunneling spectroscopy (STM), implicate PhS–Au–SPh complexes in which one gold is an adatom and the other is a surface Au atom. Crystallographic study of $Au_{102}(MBA)_{44}$ (MBA = mercaptobenzoic acid) [22] reveals a "staple" R–S–Au–SR motif (Fig. 1) in which the thiol sulfur is bound to a core and to a bridging Au atom [23], as does $[TOA^+][Au_{25}(SCH_2CH_2Ph)_{18}^-]$, where $TOA^+ = N(C_8H_{17})_4^+$ [24,25].

In the present study, the nanoparticles were prepared using the Brust method, which has very recently been shown to yield mainly Au_{38} and Au_{144} species [26]. Six different gold nanoparticle samples were prepared with the capping material ranging from pentane thiol (C_5) up to octadecanethiol (C_{18}) to observe the effect of the carbon chain on the binding and the samples were studied by far-infrared (far IR) spectroscopy.

2. Experimental

"Naked gold" particles stabilized by tetraoctylammonium bromide were prepared by reduction of $HAuCl_4$ (phase-transferred into toluene) with sodium borohydride [27]. The resulting toluene solution was washed with MilliQ water and dried with Na_2SO_4 and stored until use in a refrigerator. The rate of reaction of the particles with dodecane thiol was surveyed by monitoring the decrease in intensity of the plasmon band in a 1 mM gold solution. The absorbance change appeared biphasic, with a first half-life of ca. 1 h, followed by a ca. three times slower decrease. For the H_2 determinations portions of the "naked gold" solution were deaerated with argon and transferred to an Ar-filled glove box. Typically 0.5 mL gold stock solution was diluted with 2.0 mL 0.01 M TOAB in toluene, then 0.5 mL of 5 mM thiol in toluene containing 0.01 M TOAB was added and the stopcock was closed. The capped assemblies were removed from the glove box to determine H_2. The H_2 in the head space of the cuvettes was determined by gas chromatography on molecular sieve 5 Å (Ar carrier) [28].

The "naked gold" particles were transferred to D_2O as described by Gittins and Caruso [29] and their near-infrared-visible spectrum is presented in Fig. 2.

For the far-infrared studies the thiolate-protected gold nanoparticles were synthesized by the method of Brust et al. [15] and "annealed" as described by Murray and co-workers [31]. Solid samples were made for each of the different alkanethiols and the size distribution was calculated based on the TEM images obtained for each. The alkanethiols used (Aldrich, used without further purification) were pentane (C_5), hexane (C_6), decane (C_{10}), dodecane (C_{12}), hexadecane (C_{16}), and octadecane (C_{18}). The nanoparticle samples were stored as dried powders in the refrigerator. UV–Vis spectra of the samples are given in Fig. 3.

For the infrared work, the nanoparticle films were made just before use by applying a concentrated colloidal solution (addition of methylene chloride to the dried powder sample) dropwise onto 1 mil polyethylene film mounted in a standard FTIR sample holder and allowed to dry completely under Ar. The far-IR spectra were collected on a dry-air purged Bruker IFS-66 spectrometer equipped with a T222 mylar beamsplitter and a Far-IR DTGS detector and obtained from 200 scans at 1 cm^{-1} resolution recorded between 700 and 70 cm^{-1} at room temperature.

The transmission electron microscopy (TEM) was performed using a JEOL 100CXII instrument. As shown in Fig. 4, the average size of each of the thiolate-capped nanoparticle samples was ~2 nm in diameter, except that the decanethiol sample had a larger size (up to 20 nm) distribution than the other samples imaged.

3. Hydrogen formation in thiolate–nanoparticle assembly

Hydrogen-determination data are given in Table S1 and illustrated in Fig. 5. The reaction of the aromatic thiol, 4-methylthiophenol, was considerably more rapid than that of the C_{18} alkanethiol. In neither case is the yield quantitative: for 5-nm particles $2H_2$/Au (Eq. (2)) should be 0.17 and for 3-nm particles 0.29 is expected, but the highest value we measured was 0.1.

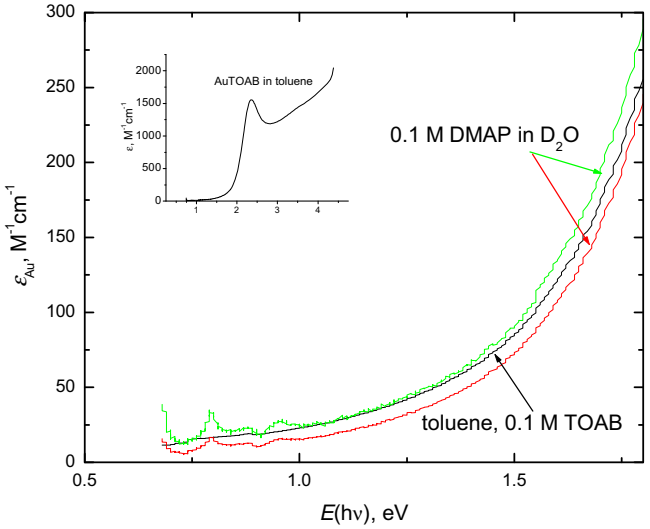

Fig. 2. Comparison of the spectra of 1–3 nm gold particles stabilized by tetraoctylammonium bromide in toluene and by dimethylaminopyridine (DMAP) in deuterium oxide. This provides evidence of only weak electronic interaction between dimethylaminopyridine adsorbate and the surface gold [30].

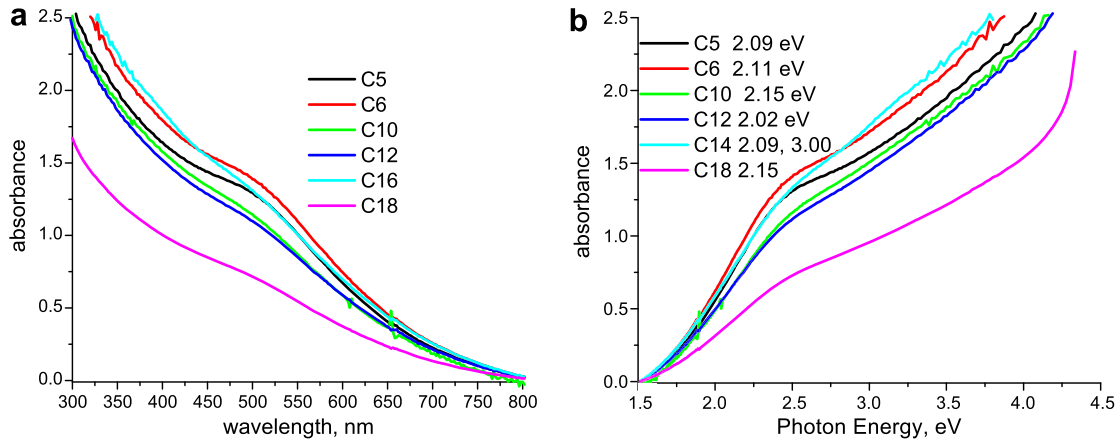

Fig. 3. UV–Vis spectra of the nanoparticles: (a) absorbance versus wavelength and (b) absorbance versus energy. The low intensity of the plasmon band indicates the size of the particle is very small. Species $Au_{144}(SR)_{39}$ and $Au_{34}(SR)_{24}$ have recently been found to predominate in the Brust prep [26]. From the electronic spectra (see Fig. 7 in Ref. [32]) Au_{144} is prevalent, consistent with ca. 2-nm particles.

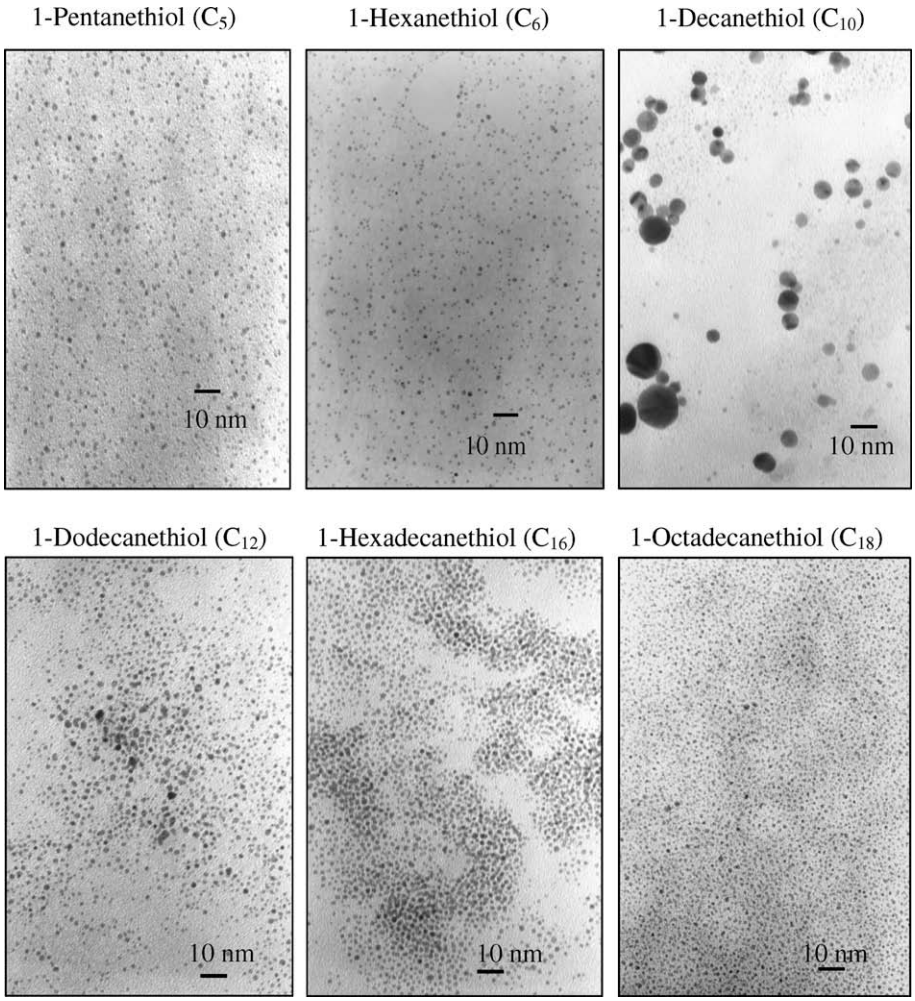

Fig. 4. TEM images of the nanoparticles.

There have now been several studies of thiolate/thiolate' replacement and thiolate–phosphine displacement on gold nanoparticles. For 1.5-nm "$Au_{101}(PPH_3)_{21}Cl_5$" displacement of the phosphine ligand was fastest for small alkanethiols (HSR), with multiphasic kinetics [33], but the fate of the hydrogen ion or atom is not known.

$$Au_{101}(PPH_3)_{21}Cl_5 + HSR \rightarrow Au_{100}(SR)_{44} + ?H_2? \quad (3)$$

For monolayer-protected clusters of aromatic thiols (HSArX) $Au_{38}(SArX)_{24}$ and $Au_{140}(SArX)_{53}$, the relatively rapid initial 25% exchange (second-order rate constant order of 10^{-3} M^{-1} s^{-1}) was attributed to associative substitution at edge/defect sites [34]. The overall process

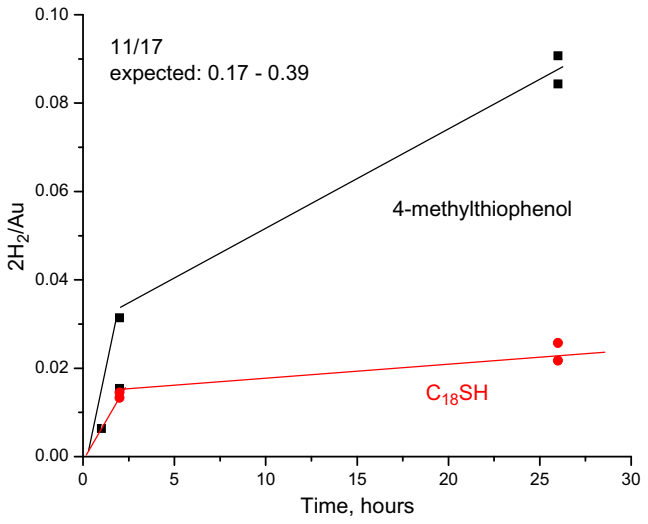

Fig. 5. Dihydrogen yield versus time for 0.8 mM thiol and 0.9 mM gold (total) in toluene containing 0.01 M TOAB.

somehow involves transfer of a proton/H-atom from the incoming to the outgoing thiol

$$Au_{38}(SArX)_{24}HSArX' \rightarrow Au_{38}(SArX')_{24} + HSArX. \quad (4)$$

The reaction studied here involves substitution of thiol on the Au surface, with redox to give H_2. The bi- or multiphasic nature of the process we observed is consistent with different reactivities for different kinds of sites on the surface, consistent with the place-exchange kinetics. The reaction is very slow, consistent with the high overvoltage for hydrogen evolution on gold [35–37]. Dihydrogen formation is much slower than the formation of thiolate-protected particles in the biphasic synthesis [15]; however, our solutions are much more dilute and thus our observations are not inconsistent with H_2 formation by the same path being operative under the synthesis conditions.

4. Far-infrared spectra of thiolate-capped nanoparticles

Fig. 6 shows the far-infrared spectrum of the C_{16} nanoparticle sample. Although the peaks are broad and the sharp bands below 400 cm^{-1} due to rotational bands of background water [38] are apparent (more apparent in some spectra than others), the peaks can still be assigned.

The slight shoulder at 642 cm^{-1} can be assigned as the C–S stretch, while the bands at 474 cm^{-1} are assigned to the C–C–C deformation and the OOP (out of plane) C–C–C deformation is attributed to the 428 cm^{-1} absorption. The S–C–C deformation is assigned to the weak band at 350 cm^{-1}. The main band at 279 cm^{-1} is attributed to the Au–S stretch.

The assignments for this sample and the other alkanethiol samples are listed in Table 1, along with data reported for KBr pellets [16] of 1.4–2.8-nm diameter gold nanoparticles of the same alkanethiols (curly brackets) and for the Au–S stretch determined by HREELS for self-assembled monolayers [39] prepared from the thiols in ethanol (square brackets).

The peaks for the C–S stretch and the deformations do not vary much with the change in the carbon chain length and they are very similar to those reported by the Murray group [16] for KBr pellets of nanoparticles of similar size. The Au–S stretching region is shown in Fig. 7 for the remaining five samples. This region shows multiple peaks at ~260, 210, and 150 cm^{-1}.

The IR spectra of the nanoparticles exhibit rather broad bands for peaks associated with binding near the nanoparticle surface [16]. They are broad (half-width ca. 50 cm^{-1}) compared to those of coordination complexes (typically 20 cm^{-1} or less). The group vibrations occurring in the far-IR region, such as the Au–S stretch, as well as the C–S stretch, the C–C–C and S–C–C deformations, are all within a bond or so away from the particle surface. Possibly the broad bands reflect local heterogeneities for different kinds of binding sites on the particle surface. A nanoparticle surface contains various types of defect sites, which can include edge, ledge, step, or kink, among others. For a 2 nm cubooctahedral particle [16], almost half (43%) of the surface atoms are proposed defect site atoms.

The far-infrared bands attributable to ν_{AuS} lie in the range 170–270 cm^{-1}, with most samples exhibiting two bands in this region. For gold alkanethiolates $Au(S{-}R)_2^-$ or $Au(S{-}R)(L)^-$, ν_{AuS} values of 220–240 [41], 280 [42], 288 (L = SCN^-) [43], 268 (L = thiourea) cm^{-1} By contrast for polymeric gold(I) thiolates AuS–R the gold–sulfur stretching bands have been assigned to a higher frequency region – between 300 and 350 cm^{-1} [44]. Vibrational spectra of small gold clusters have recently been reported to lie in the region 50–180 cm^{-1}, consistent with the low-frequency assignment (88 cm^{-1}, ν_{Au-Au}) in Table 1, but also indicating that the next higher frequencies (170, 180 cm^{-1} in the C_{16} and C_{18} species) could also arise from ν_{Au-Au} in the gold backbone [45]. Raman bands at ~270–290 and ~110 cm^{-1} have been reported for $[Au_{25}(SCH_2CH_2Ph)_{18}]^{0/1-}$ clusters [46]. The nanoparticle properties can be compared with those of 2D self-assembled monolayers (SAMs) [39,47–50]. Electron diffraction studies [51] and STM/AFM [52] have implicated thiol binding at the threefold hollow sites on Au(1 1 1). High-resolution electron energy loss spectroscopy (HREELS) studies of gold self-assembled monolayers implicate ν_{Au-S} of 220 and 240 cm^{-1} for methanethiol [13] (bound as thiol, not thiolate) and octadecanethiol [53,54], respectively, for self-assembled monolayers on Au(1 1 1). A value of 225 cm^{-1} was recently obtained from inelastic electron tunneling spectroscopy [55]. In the most comprehensive study to date Kato et al. obtained HREELS data for alkanethiolate SAMs ranging from C_2 to C_{18} [39]. The SAMs were prepared by immersion of the gold in an ethanol solution of the thiol and lack the S-H stretch. The ν_{Au-S} were found in the range 170–280 cm^{-1}, with most SAMs exhibiting two or three peaks, attributed by the authors to multiple adsorption sites [39]. The reported values are listed in Table 1 (values in square brackets) for comparison with the present results. It appears that 2D and 3D thiolates exhibit similar behavior in the ν_{Au-S} region; the observation of

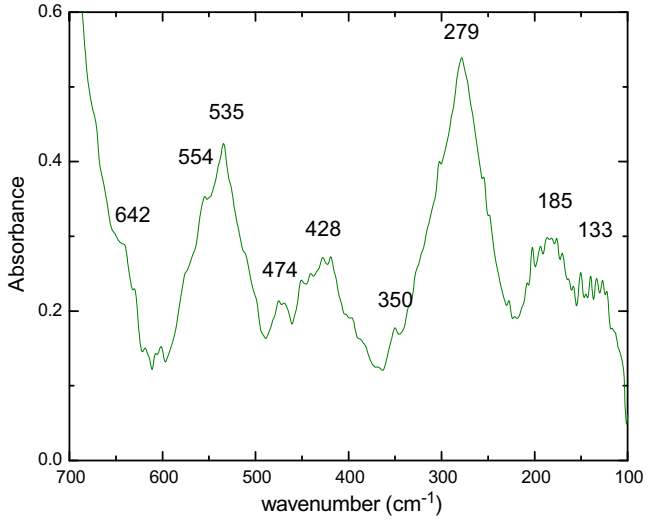

Fig. 6. Far-infrared spectrum of C_{16} thiolate nanoparticle film on polyethylene.

Table 1
Far-IR peak assignments for the alkanethiol-capped Au nanoparticles on polyethylene and comparisons with literature data for KBr pellets [16] of the nanoparticles and HREELS data [39] for self-assembled monolayers of the thiols on Au.

Assignment	C_5	C_6	C_{10}	C_{12}	C_{16}	C_{18}
C–S stretch	678[a] 640 {640}[b]	642 {642}[b]	642 608[a] {640}[b]	642 [40][b]	642 602 {645}[b]	640 604[a]
Overtones?	569	532	547	506	554 535	
C–C–C deformation	454 {457}[b]	477, 454 {482}[b] {457}[b]	476 {467}[b]	475 {463}[b]	474 {461}[b]	472
OOP C–C–C deformation		423 397	442 419 366	438 385	428	408 374
S–C–C deformation	311	304	310	320	350	329
AuS stretch	270 176	266 150 (?) [220][c]	263 170 [230][c]	271 185 [250][c] [215][c]	279 [265][c] [230][c] [180][c]	257 210 [245][c] [170][c]
Au–Au stretch?				88		89

[a] Defect site [16].
[b] KBr pellet; see Ref. [16].
[c] HREELS data from Ref. [39].

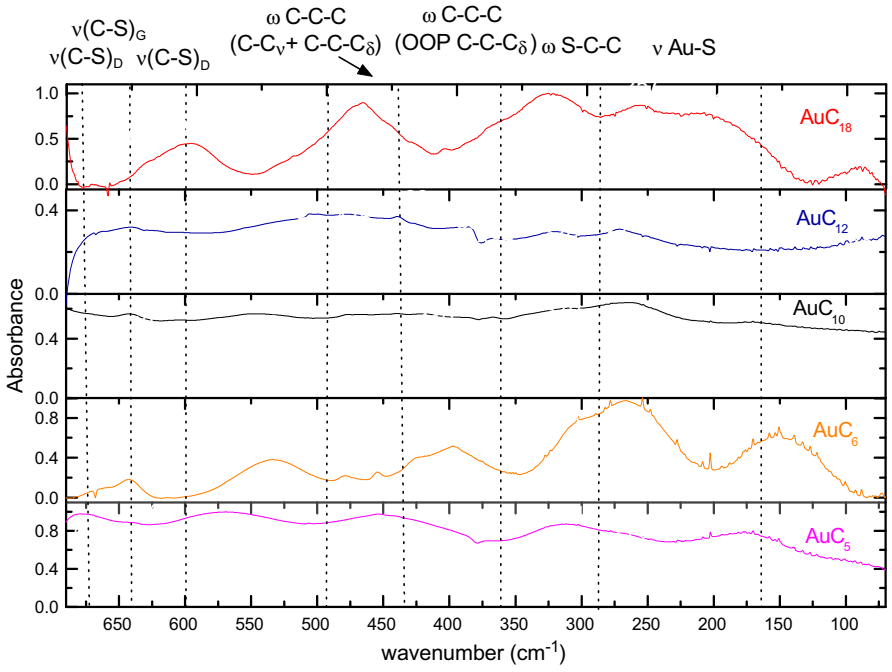

Fig. 7. Far-infrared spectra of alkanethiolate nanoparticle films on polyethylene.

multiple peaks could be associated with the recently proposed "staple" structures in which both bridging and terminal Au–SR bonds occur.

5. Concluding remarks

Hydrogen is formed (slowly) in the reaction of "naked gold" with thiols in toluene, establishing the fate of a significant fraction of the thiol H when thiols react with gold nanoparticles to yield monolayer-protected clusters. The far-infrared spectra of alkanethiolate-capped 2-nm gold nanoparticles exhibit multiple broad peaks in the Au–S stretch region leading to the conclusion of multiple binding sites or configurations of the sulfur atom to the surface gold atoms. The nanoparticles exhibit ν_{Au-S} very similar to those reported for 2D SAMs and for $Au(S{-}R)_2^-$ or $Au(S{-}R)(L)^-$ complexes consistent with recent structural models featuring an $R{-}S(Au^I(S{-}R)$ "staple" motif.

Acknowledgements

This work was performed at Brookhaven National Laboratory, funded under contract DE-AC02-98CH10886 with the US Department of Energy and supported by its Division of Chemical Sciences, Geosciences, and Energy Biosciences, Office of Basic Energy Sciences and, in part, through BNL Laboratory Research and Development funds.

Appendix A. Supplementary material

Supplementary data associated with this article can be found, in the online version, at doi:10.1016/j.jorganchem.2008.11.057.

References

[1] J.C. Love, L.A. Estroff, J.K. Kriebel, R.G. Nuzzo, G.M. Whitesides, Chem. Rev. 105 (2005) 1103–1169.
[2] C.J. Zhong, N.T. Woods, G.B. Dawson, M.D. Porter, Electrochem. Commun. 1 (1999) 17–21.
[3] M.-C. Daniel, D. Astruc, Chem. Rev. 104 (2004) 293–346.
[4] A.C. Templeton, W.P. Wuelfing, R.W. Murray, Acc. Chem. Res. 33 (2000) 27–36.
[5] M. Hasan, D. Bethell, M. Brust, J. Am. Chem. Soc. 124 (2002) 1132–1133.
[6] D. Zanchet, H. Tolentino, M.C.M. Alves, O.L. Alves, D. Ugarte, Chem. Phys. Lett. 323 (2000) 167–172.
[7] L.D. Menard, H.P. Xu, S.P. Gao, R.D. Twesten, A.S. Harper, Y. Song, G.L. Wang, A.D. Douglas, J.C. Yang, A.I. Frenkel, R.W. Murray, R.G. Nuzzo, J. Phys. Chem. B 110 (2006) 14564–14573.
[8] C.D. Bain, H.A. Biebuyck, G.M. Whitesides, Langmuir 5 (1989) 723–727.
[9] G.M. Whitesides, P.E. Laibinis, Langmuir 6 (1990) 87–96.
[10] H. Ron, I. Rubinstein, J. Am. Chem. Soc. 120 (1998) 13444–13452.
[11] W.K. Paik, S. Eu, K. Lee, S. Chon, M. Kim, Langmuir 16 (2000) 10198–10205.
[12] Y.-C. Yang, Y.-P. Yen, L.-Y.O. Yang, S.-L. Yau, K. Itaya, Langmuir 20 (2004) 10030–10037.
[13] R.G. Nuzzo, B.R. Zegarski, L.H. Dubois, J. Am. Chem. Soc. 109 (1987) 733–740.
[14] C. Kodama, T. Hayashi, H. Nozoye, Appl. Surf. Sci. 169–170 (2001) 264–267.
[15] M. Brust, M. Walker, D. Bethell, D.J. Schiffrin, R. Whyman, Chem. Commun. (1994) 801–802.
[16] M.J. Hostetler, J.J. Stokes, R.W. Murray, Langmuir 12 (1996) 3604–3612.
[17] M.A. Bryant, J.E. Pemberton, J. Am. Chem. Soc. 113 (1991) 8284–8293.
[18] A. Badia, L. Cuccia, L. Demers, F. Morin, R.B. Lennox, J. Am. Chem. Soc. 119 (1997) 2682–2692.
[19] M. Walter, J. Akola, O. Lopez-Acevedo, P.D. Jadzinsky, G. Calero, C.J. Ackerson, R.L. Whetten, H. Granbeck, H. HÅkkinen, Proc. Natl. Acad. Sci. 105 (2008) 9157–9162.
[20] N.A. Kautz, S.A. Kandel, J. Am. Chem. Soc. 130 (2008) 6908–6909.
[21] P. Maksymovych, J.T. Yates, J. Am. Chem. Soc. 130 (2008) 7518–7519.
[22] P.D. Jadzinsky, G. Calero, C.J. Ackerson, D.A. Bushnell, R.D. Kornberg, Science 318 (2007) 430–433.
[23] R.L. Whetten, R.C. Price, Science 318 (2007) 407–408.
[24] M.W. Heaven, A. Dass, P.S. White, K.M. Holt, R.W. Murray, J. Am. Chem. Soc. 130 (2008) 3754–3755.
[25] M. Zhu, C.M. Aikens, F.J. Hollander, G.C. Schatz, R. Jin, J. Am. Chem. Soc. 130 (2008) 5883–5885.
[26] N.K. Chaki, Y. Negishi, H. Tsunoyama, Y. Shichibu, T. Tsukuda, J. Am. Chem. Soc. 130 (2008) 8608–8610.
[27] J. Fink, C. Kiely, D. Bethell, D.J. Schiffrin, Chem. Mater. 10 (1998) 922–926.
[28] N.E. Katz, D.J. Szalda, M.H. Chou, C. Creutz, N. Sutin, J. Am. Chem. Soc. 111 (1989) 6591–6601.
[29] D.I. Gittins, F. Caruso, Angew. Chem., Int. Ed. 40 (2001) 3001–3004.
[30] C. Creutz, B.S. Brunschwig, N. Sutin, Chem. Phys. 324 (2006) 244–258.
[31] J.F. Hicks, D.T. Miles, R.W. Murray, J. Am. Chem. Soc. 124 (2002) 13322–13328.
[32] T.G. Schaaff, M.N. Shafigullin, J.T. Khoury, I. Vezmar, R.L. Whetten, J. Phys. Chem. B 105 (2001) 8785–8796.
[33] G.H. Woehrle, L.O. Brown, J.E. Hutchison, J. Am. Chem. Soc. 127 (2005) 2172–2183.
[34] R. Guo, Y. Song, G. Wang, R.W. Murray, J. Am. Chem. Soc. 127 (2005) 2752–2757.
[35] A.T. Kuhn, M. Byrne, Electrochem. Acta 16 (1971) 391–399.
[36] L.A. Kibler, Chemphyschem 7 (2006) 985–991.
[37] J. Greeley, M. Mavrikakis, J. Phys. Chem. B 109 (2005) 3460–3471.
[38] H.M. Randall, D.M. Dennison, N. Ginsburg, L.R. Weber, Phys. Rev. 52 (1937) 160–174.
[39] H.S. Kato, J. Noh, M. Hara, M. Kawai, J. Phys. Chem. B 106 (2002) 9655–9658.
[40] M.K. Nazeeruddin, A. Kay, I. Rodicio, R. Humphry-Baker, E. Muller, P. Liska, N. Vlachopoulos, M. Grätzel, J. Am. Chem. Soc. 115 (1993) 6382–6390.
[41] G.A. Bowmaker, B.C. Dobson, J. Chem. Soc., Dalton Trans. (1981) 267–270.
[42] R.K. Chadha, R. Kumar, D.G. Tuck, Can. J. Chem.-Revue Canadienne De Chimie 65 (1987) 1336–1342.
[43] M.M. Eletri, W.M. Scovell, Inorg. Chem. 29 (1990) 480–484.
[44] A.K.H. Al-Sa'ady, K. Moss, C.A. McAuliffe, R.V. Parish, J. Chem. Soc., Dalton Trans. (1984) 1609–1616.
[45] P. Gruene, D.M. Rayner, B. Redlich, A.F.G. van der Meer, J.T. Lyon, G. Meijer, A. Fielicke, Science 321 (2008) 674–676.
[46] J.F. Parker, J.-P. Choi, W. Wang, R.W. Murray, J. Phys. Chem. C 112 (2008) 13976–13981.
[47] T. Hayashi, Y. Morikawa, H. Nozoye, J. Chem. Phys. 114 (2001) 7615–7621.
[48] Y. Akinaga, T. Nakajima, K. Hirao, J. Chem. Phys. 114 (2001) 8555–8564.
[49] A.-S. Duwez, J. Electron Spectrosc. Relat. Phenom. 134 (2004) 97–138.
[50] F. Schreiber, Prog. Surf. Sci. 65 (2000) 151–257.
[51] L. Strong, G.M. Whitesides, Langmuir 4 (1988) 546–558.
[52] C. O'Dwyer, G. Gay, B. Viaris de Lesegno, J. Weiner, Langmuir 20 (2004) 8172–8182.
[53] A.-S. Duwez, L.-M. Yu, J. Riga, J. Delhalle, J.-J. Pireaux, J. Phys. Chem. B 104 (2000) 8830–8835.
[54] A.-S. Duwez, L.-M. Yu, J. Riga, J. Delhalle, J.-J. Pireaux, Langmuir 16 (2000) 6569–6576.
[55] W. Wang, T. Lee, M.A. Reed, J. Phys. Chem. B 108 (2004) 18398–18407.